Journal of New Materials for Electrochemical Systems 13, 271-275 (2010)

Preparation and Characterization of Ni-Mn/ZrO_2-CeO_2 Catalysts for Hydrogen Production via Methane Decomposition

M.L. Hernandez-Pichardo[1,*], M.A. Valenzuela[1], S.P. Paredes[1], P. del Angel[2] and J.A. Montoya de la Fuente[2]

[1]Instituto Politécnico Nacional-ESIQIE. Laboratorio de Catálisis y Materiales. Zacatenco, 07738, México, D. F.
[2]Instituto Mexicano del Petróleo, Dirección de Investigación y Posgrado, Eje Central L. Cárdenas 152, 07730, México, D. F.

Received: November 09, 2009, Accepted: January 29, 2010

Abstract: *Catalysts with different Ni contents supported on improved ZrO_2-CeO_2 mixed oxides and doped with manganese as a promoter of activity were evaluated on the catalytic methane decomposition (CMD) at 500 °C for hydrogen and carbon nanostructures production. The supports were synthesized by surfactant-assisted coprecipitation, and Ni and Mn deposition was performed by conventional impregnation. The surface areas for 15N1MZC and 45N1MZC solids prepared with surfactant were 13 and 28 m^2/g respectively and it was observed that by incorporating 1% of Mn to the active phase the methane conversion increases. The temperature programmed reduction results indicated that the addition of Mn allows the formation of different NiO_x species, increasing the reduction degree to Ni^0. The transmission electron microscopy analysis show the formation of different species of carbon as nanotubes, whiskers and onions, as well as an important number of encapsulated Ni particles.*

Keywords: Hydrogen Production; Catalytic Methane Decomposition; Manganese Promoter

1. INTRODUCTION

The 21st century began with an increasing demand for hydrogen in oil refining, food industry, electronic components, metallurgical processes and many others processes, though it will have the greatest impact on fuel cells [1]. The use of hydrogen in fuel cells for electricity generation has enormous potential since these systems provide efficiency as well as environmental and operational benefits over conventional technology [2]. Hydrogen is traditionally produced by steam reforming of natural gas and naphtha, heavy oil gasification and water electrolysis. In the last decade other processes such as partial oxidation, autothermal reforming and hydrocarbon decomposition have been developed [1]. Hydrocarbon decomposition is performed on either non-catalytic (thermal or plasma) or catalytic (metal or metal-based) routes [3]. The catalytic route has been focused to the decomposition of natural gas (methane) into pure hydrogen and carbon:

$$CH_{4\,(g)} \rightarrow 2H_{2\,(g)} + C_{\,(s)} \qquad (1)$$

The carbon species produced in this reaction such as nanotubes, nanofibers, and onions, offer other potential applications as electronic components, nanosensors, catalysts supports and as electrocatalytic supports for fuel cells [2,4].

Transition and noble metals such as Ni, Fe, Pd and Co, supported on alumina or silica have been extensively studied as potential catalysts for CMD [5] and references therein; although carbon-based materials have also been tested for this purpose. However, among all catalysts investigated, nickel emerges to impart the highest activity. Unfortunately, rapid deactivation of Ni-based catalyst results at temperatures in excess of 600 °C, leading to a low yield of hydrogen. Therefore, studies on the development of more stable Ni catalysts are needed.

It has been reported that it is possible to obtain high methane conversions to produce hydrogen and carbon nanotubes by CMD using Ni catalysts supported on ZrO_2-CeO_2 mixed oxides, although the deactivation by carbon deposits on the surface remains as problem in the stability of these catalysts, despite the high resistance to coke deposit of these materials [6]. However, some research works have shown that doping nickel with a second component such as Fe, Cu and Mn, enhances the activity and stability of Ni catalysts on oxides such as Al_2O_3, CeO_2 or ZrO_2 pure oxides [7-10]. Then, this study aims to evaluate the effect of the incorporation of manganese as a dopant in Ni catalysts supported on ZrO_2-CeO_2 mixed oxides for the CMD to increase hydrogen yield and stability of Ni

*To whom correspondence should be addressed: Email: mhernandezp@ipn.mx
Phone: (+) 52 55 57 29 60 00; Fax: (+) 52 55 86 27 28

particles. Mn has been used as a dopant in Ni-Mn/ZrO_2 [8] and Ni-Mn/TiO_2 [11] catalysts showing high activity for the CMD; however, it has not yet been established the effect of Mn addition on Ni/ZrO_2-CeO_2 catalysts.

Furthermore, although ZrO_2-CeO_2 supports present good reducibility properties, its surface area is very low which limits the metal dispersion on the surface [12]. Therefore, in this work ZrO_2-CeO_2 supports were synthesized by surfactant-assisted coprecipitation in order to improve the textural properties of these materials.

2. EXPERIMENTAL

2.1. Catalysts Preparation

ZrO_2-CeO_2 oxides (80 wt.% ZrO_2-20 wt.% CeO_2) used as supports were prepared by surfactant-assisted coprecipitation from chemicals provided by Aldrich. The surfactant used was an aqueous solution (0.4 M) of cetyl-trimethylammonium bromide (CTAB). These supports were prepared using zirconyl chloride $ZrOCl_2 \times xH_2O$ and cerium (III) nitrate hexahydrate $Ce(NO_3)_3 \cdot 6H_2O$ chemicals. Aqueous solutions of zirconyl chloride (0.3 M), and cerium nitrate (0.3 M) were mixed with the CTAB solution. This solution was stirred for 2 h at 60 °C, and then NH_4OH was added to reach a pH 11. The precipitates were washed repeatedly and then dried at 110 °C for 16 h. The calcination treatment was performed in static air at 800 °C for 4 h.

The ZrO_2-CeO_2 supports were impregnated with Ni ($Ni(NO_3)_2 \cdot 6H_2O$) at different compositions (15 and 45 wt.%) and another series with 1 wt.% Mn ($Mn(NO_3)_2 \cdot xH_2O$). The impregnated solids were then dried at 110 °C for 16 h and finally calcined in static air at 400 °C during 4 h. The catalysts description and the nomenclature used are described in Table 1.

2.2. Catalyst characterization

Ni/ZrO_2-CeO_2 and Ni-Mn/ZrO_2-CeO_2 catalysts were characterized by diverse techniques. X-ray diffraction patterns were obtained in a Bruker-Axs D8 Discover with GADDS (General Area Detector Diffraction Systems, two-dimensional detector) diffractometer fitted with a Cu tube (40 kV, 40 mA) using HTE approaches for both, measurements, and patterns evaluation. The mean particle dimension was calculated with respect to intensity for the main diffraction line using Scherrer equation and the full half width of the characteristic peak of each XRD pattern. These materials were studied by HRTEM using a JEOL JEM2200FS microscope with Schottky type field emission gun, operating at 200 kV and integrated with a CEOS aberration corrector. The elemental composition was determined by EDS with a NORAN spectrometer fitted to the TEM. In order to prepare the materials for observation, the powder samples were dispersed in ethanol and supported on holey carbon coated copper grids. HRTEM digital images were obtained using Digital Micrograph Software from GATAN. Finally, temperature programmed reduction (TPR) analyses were conducted in a Micromerirtics TPD/TPR equipped with a conductivity detector. The reduction was carried out by using 50 mg sample from 30 to 900 °C (10 °C/min) using a 5% H_2/Ar mixture. The BET analyses were also performed in a Micromerirtics TPD/TPR equipment, prior to the measurements the samples were out-gassed at 350 °C for 2 h in vacuum.

Table 1. Composition and nomenclature used for the synthesized catalysts

Catalyst	% Ni	% Mn
15NZC	15	0
45NZC	45	0
15N1MZC	15	1
45N1MZC	45	1

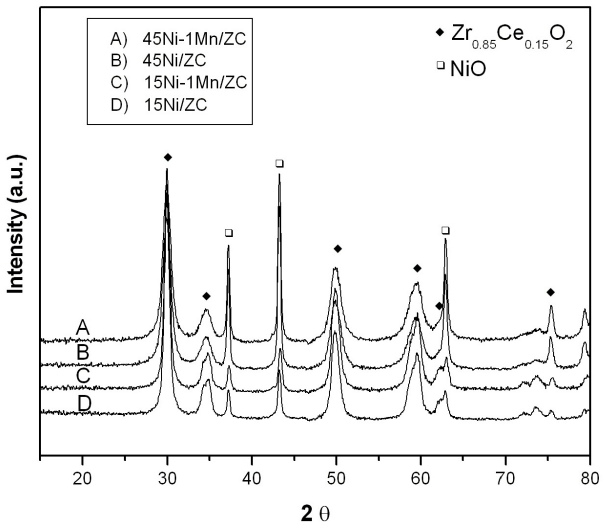

Figure 1. XRD spectra of Ni/ZrO_2-CeO_2 and Ni-Mn/ZrO_2-CeO_2 catalysts calcined at 800 °C.

2.3. Catalytic testing

Catalytic activity was measured in the methane decomposition reaction over the Ni-Mn/ZrO_2-CeO_2 catalysts. This evaluation was accomplished in a stainless steel microreactor (Advanced Scientific Designs, RXM-100). This reaction system consists of a microreactor of approximately 4 mm of inner diameter and 15 cm length. The reactor heads is connected to an Agilent gas chromatograph (Agilent 6890) equipped with a capillary column Molosieve (Perkin Elmer), a thermal conductivity detector, TCD (H_2) and a flame ionization detector, FID (CH_4) for the analysis of products. A catalyst sample of 100 mg was loaded into the reactor and the pretreatment of the catalysts was carried out in situ prior to the activity test. The pretreatment consisted in a drying-reduction program, drying the samples at 100 °C for 1h in Ar (70 $cm^3 min^{-1}$) followed by reduction in a hydrogen flow (30 $cm^3 min^{-1}$) at 500 °C for 1 h. The reaction was conducted at 500 °C and using a mixture of 10% CH_4-90% Ar in volume at atmospheric pressure.

3. RESULTS AND DISCUSSION

3.1. Crystalline Structures of Catalysts

The crystalline structure of Ni/ZrO_2-CeO_2 and Ni-Mn/ZrO_2-CeO_2 catalysts calcined in air at 800 °C were examined by X-ray diffraction. As shown in Figure 1 the identification of the crystalline phases indicates that the surfactant-assisted coprecipitation allows the formation of $Zr_{0.85}Ce_{0.15}O_2$ mixed oxides in cubic phase, with

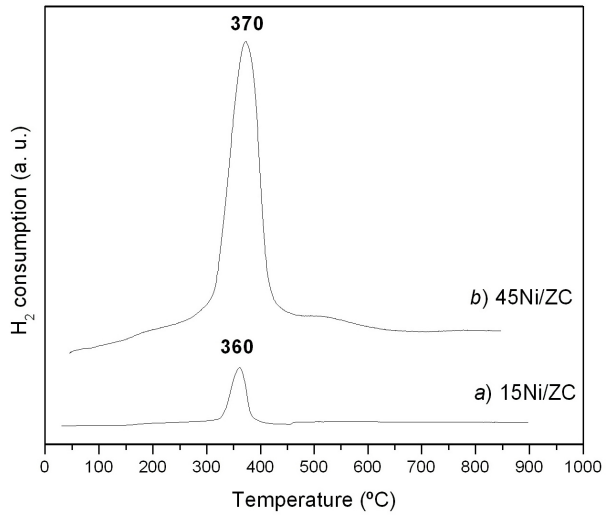

Figure 2. TPR profiles of 15% Ni/ZrO_2-CeO_2 and 45Ni/ZrO_2-CeO_2 catalysts. Effect of the Ni content.

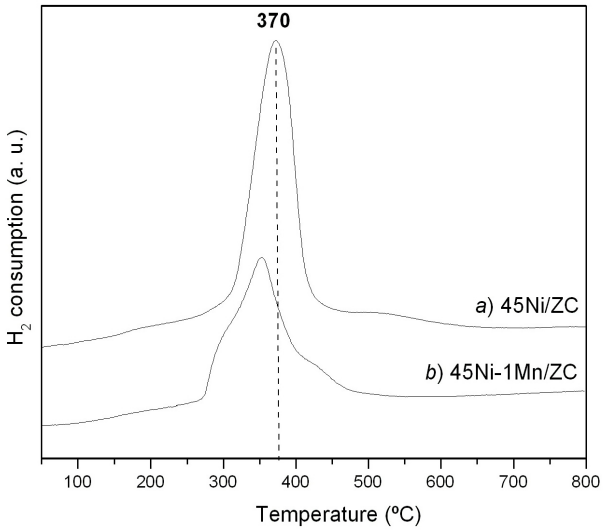

Figure 3. Effect of manganese incorporation in the reducibility of the 45% Ni/ZrO_2-CeO_2 Catalyst.

main diffractions at 2θ = 30, 35, 50 and 60; it has been reported that the cubic phase of ZrO_2-CeO_2 presents higher oxygen storage capacity (OSC) and that it is it is easily reduced than the tetragonal phase [13]. These patterns do not present the corresponding reflections of ceria or zirconia, indicating the formation of a solid solution, since there is no segregation of these simple oxides in these materials.

A comparison of patterns with different Ni content shows the expected rise of the intensities of the reflections corresponding to NiO at 2θ = 37, 43 and 63, with increasing nickel content. It is noted that these reflections are very narrow indicating that by this synthesis method very large NiO particles were obtained. The NiO crystallite size measurements calculated with the Scherrer equation indicate that an average size of about 26 nm was obtained, except for 15N1MZC catalyst which showed a particle size smaller than 21 nm (Table 2). It was also observed a slight broadening of the reflections of the support with the increase of Ni content at 45%, suggesting a slight reduction of crystallinity and particle size of these materials, which is confirmed by measuring the particle size (Table 2). It is important to note that these analyses were obtained in combinatorial equipment under identical conditions, so that the diffraction peaks can be compared directly in position and intensity. Finally the comparison of diffractograms of samples with and without manganese showed no structural differences with the incorporation of this ion to the catalytic system.

Table 2. Average crystallite size determined from XRD patterns by Scherrer equation

Catalyst	d_{NiO} (nm)	$d_{ZrO_2-CeO_2}$ (nm)
15NZC	25.97	13.85
15N1MZC	20.73	12.81
45NZC	25.97	8.23
45N1MZC	25.97	8.56

3.2. Reduction of nickel metal precursor species

The reducibility of the catalysts was studied by TPR. Figure 2 shows the hydrogen consumption profiles of the catalysts with 15 and 45% Ni. Reduction peaks were observed around 300–450 °C; the reduction profile of the catalyst with 15% Ni presented a small hydrogen consumption at 360 ºC associated with the reduction of Ni ($Ni^{II} \rightarrow Ni^0$), while for the catalyst with 45% Ni the hydrogen consumption increased significantly at about the same temperature, which confirms that this reduction peak is due to the reduction of NiO. It is well known that the pure nickel oxide is reduced between 330 and 430 °C [14], then, our results indicate that the Ni impregnation over the mixed oxide $Zr_{0.85}Ce_{0.15}O_2$ generates a weak interaction with the support, favoring the reducibility of the supported NiO.

The effect of the incorporation of Mn in the reducibility of these catalysts is shown in Figure 3. It is observed that both catalysts with the same Ni content (45%) show similar reduction profiles, however the Mn incorporation brings about reduced hydrogen consumption and a widening of the reduction band at about 350 ºC, suggesting that manganese oxides enhance the reduction of NiO. In addition these profiles show that the catalyst with Mn presents two shoulders on the sides of the maximum peak (at 350 ºC), widening the temperature range of the reduction, which could indicate that the addition of Mn induces to the formation of a variety of NiO_x sites, which interact in different extents with the support. These different H_2 consumption regions may be due then to the reduction of Ni^{2+} on the surface, and the peak a higher temperature could be attributed to the reduction of the Ni species with a higher interaction with the support. Furthermore, the shoulder at 300 °C can be attributed to the reduction of manganese species, particularly to the reduction of Mn_2O_3, since it has been found that this oxide is reduced at this temperature [15], and under these synthesis conditions (calcination at 800 °C), this is the most probable oxide that could be mainly found in these catalysts. Thus, the use of this promoter affects the redox properties of the catalyst allowing that the reduc-

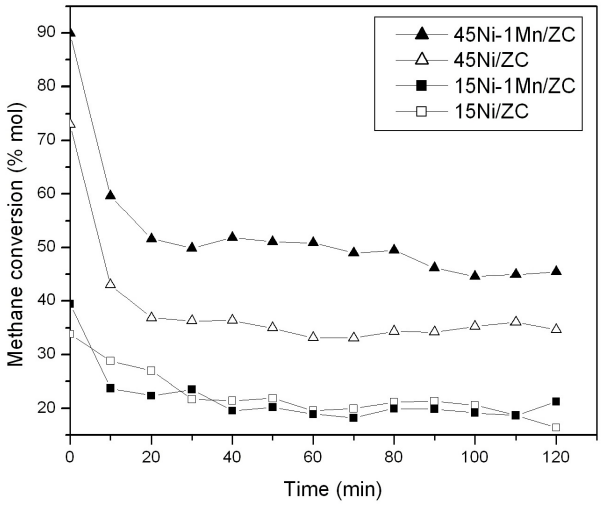

Figure 4. Catalytic activity of Ni/ZrO_2-CeO_2 and Ni-Mn/ZrO_2-CeO_2 samples in the CMD at 500 º C with different Ni and Mn contents.

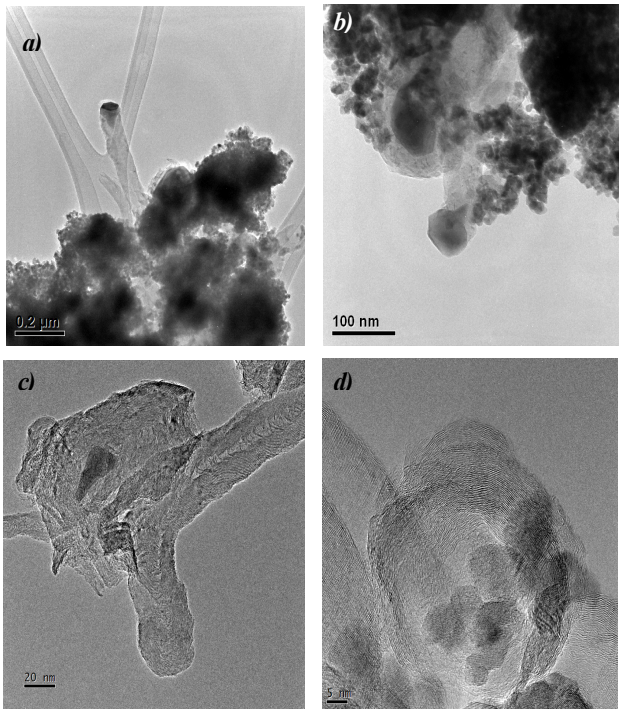

Figure 5. Typical electron microscopy images of samples after reaction in DCM at 500 º C: a) and b) low magnification images; c) and d) HRTEM images.

tion processes are carried out at lower temperatures, as it has been found with other promoters [10,16].

3.3. Catalytic activity

The results of the catalytic evaluation of Ni/ZrO_2-CeO_2 and Mn-dopped samples in the catalytic decomposition of methane (CMD) to produce hydrogen and carbon at 500 ºC are shown in Figure 4. As expected, an increase in nickel content leads to an increase in the catalytic activity of these materials. In this plot is clearly noted that the Mn incorporation produces a higher initial conversion and an increase of 12% in methane conversion with 45% Ni catalysts. The comparison of the catalytic activity of these samples in terms of the methane conversion, indicates that the incorporation of 1% of manganese leads to an increase in the activity of catalysts with higher nickel content, this behavior can be attributed to the different Ni surface species generated with the Mn incorporation, having different interactions with the support, as shown in Figure 3, which generate greater reducibility of these materials, even at lower temperatures. This enhanced reducibility at low temperature causes a high activity in these catalysts; in this sense, it is also possible that the surfactant-assisted synthesis produces a higher surface area and porosity in the samples, allowing a better diffusion of reactants in the catalyst; the surface areas for 15N1MZC and 45N1MZC catalysts prepared with surfactant were 13 and 28 m^2/g respectively that are superior values to those reported for catalysts calcined at 800 °C prepared by conventional methods without surfactant [17]; these results show the advantage of the surfactant-assisted method to obtain catalysts with higher surface area. Then, the role of Mn in the whole catalytic system may be to modify the Ni species produced on the surface, either by a geometric effect of particle decoration, or to modify the Ni interaction with the support when manganese is incorporated preferentially into the ZrO_2-CeO_2 lattice.

In all cases the catalysts were deactivated rapidly to about half of the value of the initial conversion, achieving stabilization at approximately 30 min of reaction. The main reported reason for deactivation is the coke deposition on the Ni active phase. Due to the deactivation profiles were similar with or without Mn addition, it is concluded that its incorporation only has a significant effect on initial rate of methane decomposition.

3.4. Characterization of the different carbon nanostructures formed after reaction

The type of carbon nanostructures formed on these materials after the reaction on DCM was studied by TEM and XRD; the results of the study by TEM are shown in Figure 5. It is possible to observe that after the reaction for 2 h different carbon structures are formed, both amorphous and crystalline, from the formation of nanotubes and whiskers (Figures 5a and 5b) to the formation of concentric onion structures (5c and 5d). In all cases it was observed that there is a high concentration of Ni particles at very different particle sizes encapsulated with carbon that is the main cause of deactivation. It is found that the type of carbon species formed depends on several factors such as the kind of support [10], the synthesis method [11], reaction conditions [18] and even the nickel content on similar catalysts [19]. The activity of this kind of catalysts changes due to carbon formation mechanism [17], according to the HRTEM results, the Mn incorporation modifies the interaction of Ni with the support, this allows the formation of various carbon nanostructures that modify the catalytic performance of these materials. According to the well know mechanism of the carbon formation [20], the diffusion of carbon through nickel modifies the nickel–carbon interface separating the Ni particle trough the formation of whiskers with the Ni particle in the end (Figure

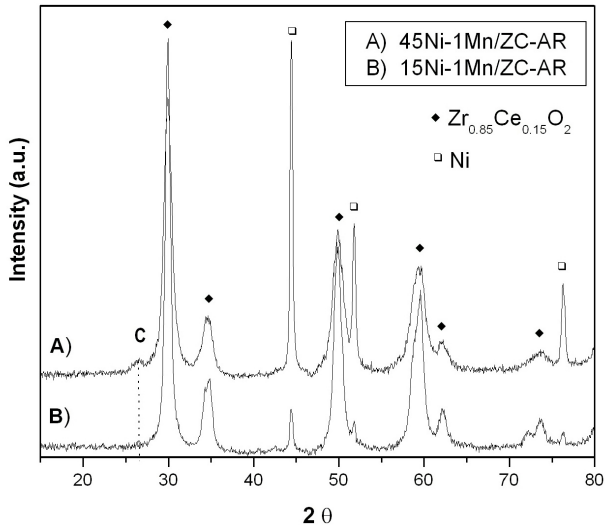

Figure 6. Carbon identification by X-ray diffraction patterns of Ni-1Mn/ZrO_2-CeO_2 catalysts after reaction (AR) in CMD at 500 ºC.

5a) that allows the permanence of Ni on the surface and thus the stability of the catalytic activity. However if this process is not completed, the carbon begins to cover the nickel particle encapsulating it and forming onion-like structures around Ni particle, deactivating the catalysts. From the HRTEM results it was observed that the metal particles at the end of the filaments were not present at the whole surface and in the unpromoted catalysts a higher combination of the encapsulated Ni particles and onion structures was observed (Figure 5b).

Finally, we observed that using catalysts with high Ni content the formation of crystalline carbon was observed, which was identified by XRD (Fig. 6) with the formation of the diffraction at 2θ = 26, which corresponds to the main peak of graphite with planes [0 0 2], which confirms a higher formation of graphitized carbon in catalysts with higher Ni content. The particle size of nickel crystals was determined using the Scherrer equation using the reflection [1 1 1] at 2θ = 44.4 from the diffraction patterns of catalysts after reaction. This analysis showed a slight decrease in the particle size of Ni^0 with the addition of manganese in the case of the catalyst with 45% Ni from 30 to 27 nm which is in fact to small to be considered as a Mn effect and it is definitely on the experimental error; however, the change in the particle size was also observed by HRTEM since the particle size measured by XRD in these materials is complex due to this is a high-symmetry cubic system and thus the reflections are very narrow and intense, and the signals from smaller particles almost do not contribute to the total reflection. Still, the results showed a decrease in particle size also observed qualitatively by HRTEM, but it can be directly attributed to Mn.

4. CONCLUSIONS

Preliminary studies of Mn-dopped Ni/ZrO_2-CeO_2 catalysts showed that the incorporation of Mn increases the reducibility of these catalysts probably through the formation of different NiO_x species that interact differently with the support. Mn addition caused a significant effect of the initial rate of decomposition of methane; however the deactivation behavior was not improved in comparison with Ni catalysts. Different types of nanostructured carbon (nanotubes, whiskers and onions) were formed, which could be explained in terms of the metal-support interactions after incorporation of Mn. Moreover, it was found that the synthesis of these catalytic materials using a surfactant-assisted method generates a positive effect on the activity of these catalysts, probably due to an increase in the surface area and porosity that allows a higher diffusion of reactants.

5. ACKNOWLEDGMENTS

The authors thank to the Instituto Politecnico Nacional for the financial support granted for the development of this work.

REFERENCES

[1] P.K. Cheekatamarla, C.M. Finnerty, J. Power Sources, 160, 490 (2006).
[2] D. Sebastian, I. Suelves, M.J. Lazaro, R. Molinera, J. Power Sources, 192, 51 (2009).
[3] S. Ahmed, A. Aitani, F. Rahman, A. Al-Dawood, F. Al-Muhaish, Appl.Catal. A, 359, 1 (2009).
[4] Suelves, J.L. Pinilla, M.J. Lazaro, R. Moliner, Chem. Eng. J., 140, 432 (2008).
[5] R.M. Navarro, M.A. Peña, J.L.G. Fierro, Chem Rev., 107, 3952 (2007).
[6] W. Dong, K. Jun, H. Roh, Z. Liu, S. Park, Catal. Lett., 78, 215 (2002).
[7] J. Chen, Y. Qiao, Y. Li, Appl. Catal. A, 337, 148 (2008).
[8] S. Kurasawa, S. Iwamoto, M. Inoue, Mol. Cryst. Liq. Cryst., 387, 123 (2002).
[9] T.V. Reshetenko, L.B. Avdeeva, Z.R. Ismagilov, A.L. Chuvilin, V.A. Ushakov, Appl. Catal. A, 247, 51 (2003).
[10] A. Trovarelli, Catal. Rev., 38, 439 (1996).
[11] S.H.S. Zein, A.R. Mohamed, P.S.T. Sai, Ind. Eng. Chem. Res., 43, 4864 (2004).
[12] V.B. Mortola, J.A.C. Ruiz, L.V. Mattos, F.B. Noronha, C.E. Hori, Catal. Today, 133, 906 (2008).
[13] H. Roh, K. Jun, W. Dong, S. Park, Y. Baek, Catal. Lett., 74, 31 (2001).
[14] R. Brown, M.E. Cooper, D.A. Whan, Appl. Catal, 3, 177 (1982).
[15] E.R. Stobbe, B.A. de Boer, J.W. Geus, Catal. Today, 47, 161 (1999).
[16] F. Arena, G. Trunfio, J. Negro, L. Spadaro, Mat. Res. Bull., 43, 539 (2008).
[17] J.A. Montoya, E. Romero-Pascual, C. Gimon, P. Del Angel, A. Monzón, Cat. Today, 63, 71 (2000).
[18] Y. Zhang, K.J. Smith, Catal. Today, 77, 257 (2002).
[19] C.N. He, N.Q. Zhao, X.W. Du, C.S. Shi, J.J. Li, F. He, Mat. Sci. Eng. A-Struct., 479, 248 (2008).
[20] J.W. Snoeck, G.F. Froment, M. Fowlest, J. Catal., 169, 240 (1997).